Supplementary Information

Highly graphited carbon-coated $FeTiO_3$ nanosheets *in situ* derived from MXene: an efficient bifunctional catalyst for Zn-air batteries

*Yingxinjie Wang, Jie Zhu, Yan Jiang, Tianyun An, Jingbin Huang, Minxia Jiang and Minhua Cao**

Key Laboratory of Cluster Science, Ministry of Education of China, Beijing Key Laboratory of Photoelectronic/Electrophotonic Conversion Materials, School of Chemistry and Chemical Engineering, Beijing Institute of Technology, Beijing 100081, P. R. China.

*Corresponding author: E-mail: caomh@bit.edu.cn

Experimental section

Materials

Ti_3AlC_2 powder (> 98 wt%) was obtained from Institute of Metal Research, Chinese Academy of Science, Shenyang. Lithium fluoride (LiF, 98+%) was purchased from Alfa Aesar. Hydrochloric acid (36-38 wt%) was purchased from Beijing Chemical Works. Hexadecyl trimethyl ammonium bromide (CTAB, ≥ 99. 0%) was purchased from Sinopharm Chemical Reagents Co., Ltd. All chemicals used in the experiments were analytical grade without further purification.

Preparation of $Ti_3C_2T_x$ nanosheets

$Ti_3C_2T_x$ was prepared based on the previous work.[1] Firstly, 0.998 g of LiF was dissolved in 10 mL of HCl (9.0 mol L^{-1}) under stirring. Secondly, 1.0 g of Ti_3AlC_2 powder was slowly added into the above solution, followed by stirring for 24 h at 36 ^oC to remove the Al layer of Ti_3AlC_2. After etching for 24 h, the multilayer $Ti_3C_2T_x$ was washed with deionized water and centrifuged (3500 rpm, 5 min) until pH was above 6. Then, the as-obtained wet multilayer $Ti_3C_2T_x$ sediment was redispersed into 20 mL of deionized water and sonicated for 1 h with ice bath under inert atmosphere. Finally, the $Ti_3C_2T_x$ nanosheet supernatant was obtained by centrifuging at 3500 rpm for 1 h.

Preparation of $FeTiO_3$@C nanosheets

Before the preparation of $FeTiO_3$@C nanosheets, we need to thermally treat a 5 mL of stainless steel reactor (316L type stainless steel) was calcined in a muffle furnace at 800 ^oC for 2 h, which then was washed with deionized water for several times. Subsequently, the as-treated reactor was filled with deionized water, and soaked for different times (2, 6, and 18 h) to control the extent of the rust formed. Finally, the reactor was dehydrated in an oven at 60 ^oC to obtain the rusted -reactor.

For a typical synthesis for $FeTiO_3$@C nanosheets, firstly, 15 mmol of hexadecyl

trimethyl ammonium bromide (CTAB) was dissolved in 60 mL of deionized water under vigorous stirring until forming a clear solution. Then, 10 mL of $Ti_3C_2T_x$ suspension solution obtained above was dropwise added into the above solution, followed by stirring for 30 min at the ice bath. After that, the mixed suspension was dried under vacuum freeze-drying for 72 h to obtain the precursor for $FeTiO_3$@C. Subsequently, in an argon-filled glovebox, the precursor powder was transferred into a rusted-reactor (after being soaked for 6 h), followed by storing in muffle furnace at 500 ^oC for 24 h, and the obtained sample was named as $FeTiO_3$@C. In addition, $FeTiO_3$@C-T (T = 400, 450 and 550 ^oC) were also prepared at different annealing temperatures. If we used the rusted-reactor that has been soaked for different times (2 and 18 h), the products obtained by calcination at 500 ^oC for 24 h were named as $FeTiO_3$@C-2 h and $FeTiO_3$@C-18 h.

Materials characterizations

The morphology and structure of the samples were examined by using field emission scanning electron microscopy (FE-SEM; JEOL S-4800) and transmission electron microscopy (TEM; JEOL JEM-2010) as well as high-resolution TEM (HRTEM). The crystal structure was measured by using powder X-ray diffraction (XRD; Bruker D8 Advance Diffractometer) with Cu-Kα radiation ($\lambda \approx 0.154$ nm) at 40 kV and 40 mA in the scanning range of 5°-80°. Raman spectra were collected on an Invia Raman spectrometer with an excitation laser wavelength of 532 nm. Nitrogen adsorption/desorption curves were measured by using the Barrett-Joyner-Halenda (BJH) and Brunauer-Emmett-Teller (BET) method to calculate the specific surfaced area of the samples under N_2 physisorption at 77 K. X-ray photoelectron spectroscopy (XPS) was exploited to study the chemical states by using an ESCALAB 250 spectrometer (PerkinElmer), and the C 1s level at 284.8 eV was taken as a reference to calibrate the binding energies. The thermogravimetric analysis (TGA) was performed from room temperature to 650 ^oC in an air atmosphere with a rate of 10 ^oC min^{-1} by using a DTG-60AH instrument.

Electrochemical measurements

Preparation of electrocatalyst ink

The working electrode, as a homogeneous ink, for electrochemical measurements was prepared by 4 mg of dispersing the as-prepared catalyst powder into 1 ml of ethanol solution and 20 μL of 0.5 wt% Nafion solution, followed by ultrasonication for 30 min. Then, 20 μL of the above slurry was coated onto a glassy carbon electrode with a diameter of 3 mm or 5 mm and dried naturally under room temperature for later OER or ORR test.

OER and ORR measurements

The OER and ORR electrochemical tests were prepared in a CHI 760E electrochemical workstation (CH instrument, Chenhua, China) using a standard three-electrode cell. Among them, a Hg/HgO electrode and a graphite rod were used as the reference electrode and the counter electrode, respectively. All current densities were normalized to the geometrical surface area and the measured potential *vs.* Hg/HgO (1 M KOH) was converted to the potential vs. the reversible hydrogen electrode (RHE) according to the Nernst equation E(RHE) = E(Hg/HgO) + 0.098 + 0.0592pH. Linear sweep voltammetry (LSV) measurements were executed to obtain the polarization curves at a scan rate of 5 mV s^{-1} in a O_2-saturated 1M KOH aqueous electrolyte. The Tafel slope was calculated from the corresponding LSV curves according to Tafel equation $\eta = b \log(j/j_0)$.[2] Electrochemical surface areas (ECSA) were obtained by testing the electrochemical double-layer capacitance (C_{dl}) from cyclic voltammetry (CV) at non-faradaic overpotentials. By plotting the difference value in current density between the anodic and cathodic sweeps (ΔJ) at a specific potential against the CV scan rate, a linear trend was observed. The linear slope, equivalent to twice of C_{dl}, was used to represent the ECSA. Electrochemical impedance spectroscopy (EIS) was measured at a potential of 10 mA/cm^{-2} with the frequency range from 100 KHz to 0.01 Hz with an amplitude of 5 mV. The long-term durability was tested by a chronoamperometric

curve at a potential of 10 mA/cm^{-2}. All the data measured were not using the IR compensation.

The ORR electrochemical test was similar to that of OER. The electrochemical experiments were carried out in O_2-saturated 0.1 M KOH electrolyte for the oxygen reduction reaction. The potential range is cyclically scanned between 0.2 and 1.0 V *vs.* RHE with a scan rate of 5 mV s^{-1} or 10 mV s^{-1} in order to obtain the LSV or CV in ORR. In the meantime, the potential cycling was repeated until stable voltammogram curves were obtained.

The rotating ring-disk electrode (RDE) tests were carried out at various rotating speeds from 400 to 2025 rpm at a scan rate of 5 mV s^{-1}. The exact kinetic parameters were calculated on the basis of Koutecky-Levich equations as follows[3]:

$$\frac{1}{J} = \frac{1}{J_k} + \frac{1}{(B\omega^{1/2})} \quad (1)$$

$$B = 0.2nFC_o D_o^{2/3} \upsilon^{-1/6} \quad (2)$$

$$J_k = nFkC_o \quad (3)$$

in which J is the measured current density, J_k is the kinetic current density, ω is the rotation speed (the constant 0.2 is used when the rotation rate is expressed in rpm), n is the transferred electron number, F is the Faraday constant (F = 964 85 C mol^{-1}), C_o is the concentration O_2-saturated in the electrolyte (1.21×10^{-3} mol L^{-1}), D_o is the diffusion coefficient of O_2 in the solution (1.9×10^{-5} cm^2 s^{-1}), υ is the kinetic viscosity of the electrolyte (0.01 cm^2 s^{-1}), and k is the electron-transfer rate constant.

Zn-air battery measurements

We assembled and tested the rechargeable Zn-air batteries (RZABs), in which the prepared $FeTiO_3$@C-T catalyst was sprayed onto carbon paper as the air cathode (the loading of catalyst is 5 mg cm^{-2} and the coating area of the catalyst is 1×1 cm^{-2}), a polished Zn plate was used as the anode and 6 M KOH aqueous solution was utilized as the electrolyte. The cycling test of the RZABs was monitored by LAND CT2001 A instrument, in which one cycle consisted of a discharge process at a current density of

10 mA cm^{-2} for 10 min followed by charging under the same conditions. The charging and discharge polarization curves of the RZABs were performed by electrochemical workstation (CHI 760D). All electrochemical tests were performed at room temperature and atmospheric pressure.

Supplementary Figures

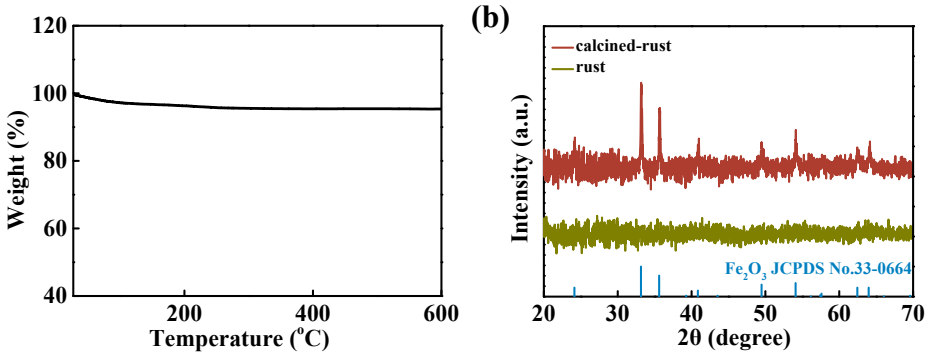

Fig. S1 (a) TGA curve of the rust under air atmosphere. (b) XRD patterns of the rust before and after calcining at 400 °C.

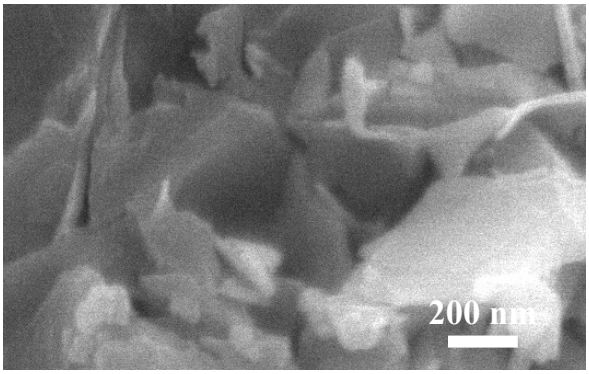

Fig. S2 FE-SEM image of $FeTiO_3$@C.

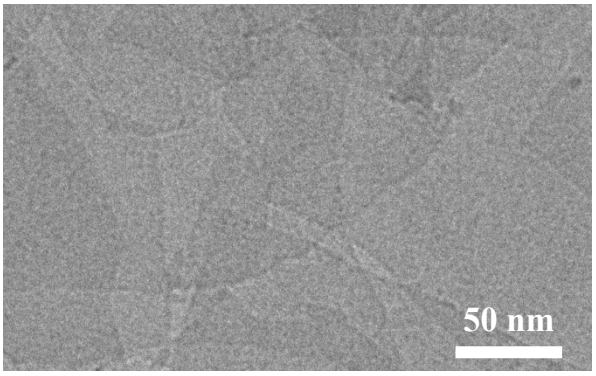

Fig. S3 TEM image of $Ti_3C_2T_x$.

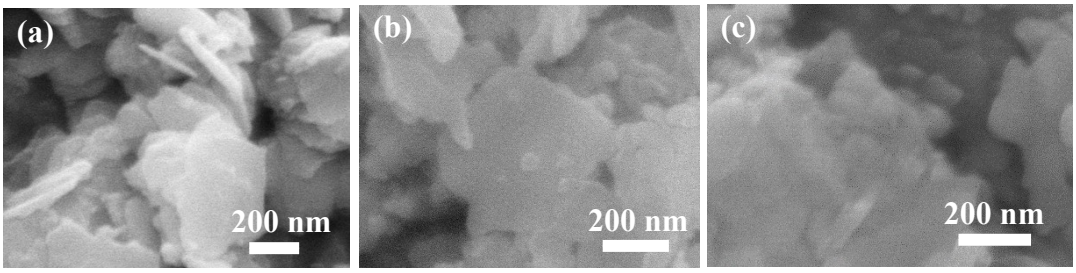

Fig. S4 FE-SEM images of (a) $FeTiO_3$@C-400, (b) $FeTiO_3$@C-450 and (c) $FeTiO_3$@C-550.

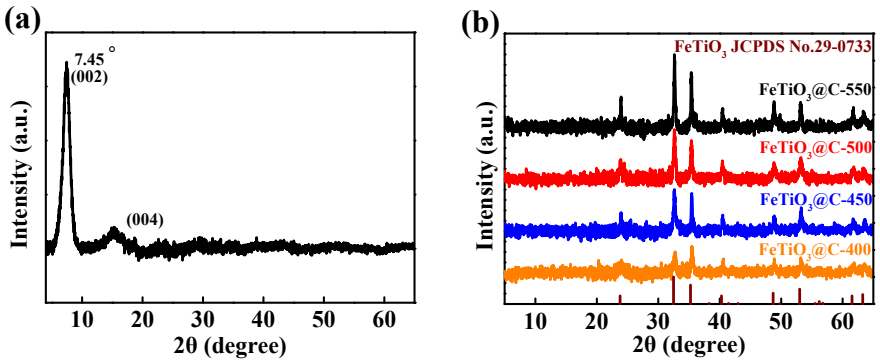

Fig. S5 XRD patterns of (a) $Ti_3C_2T_x$ and (b) $FeTiO_3$@C-T samples.

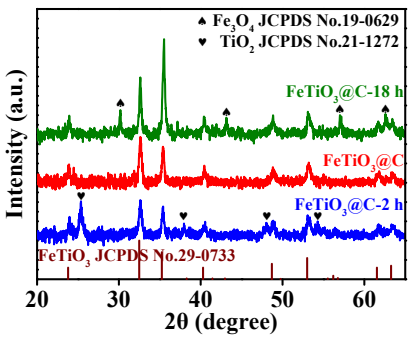

Fig. S6 XRD patterns of the $FeTiO_3$@C, $FeTiO_3$@C-2 h, and $FeTiO_3$@C-18 h.

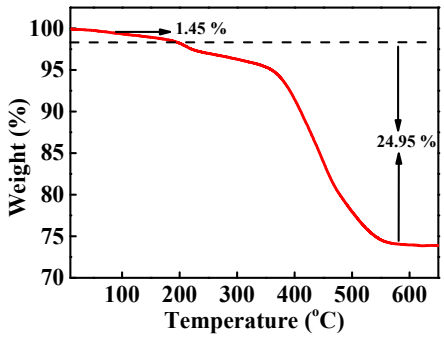

Fig. S7 TGA curve of $FeTiO_3$@C under air atmosphere.

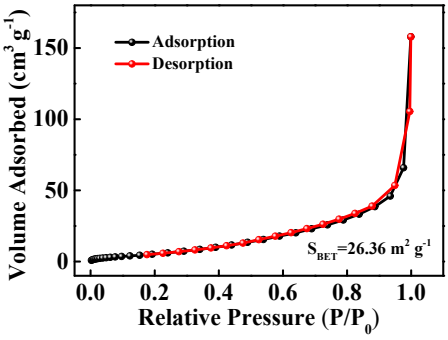

Fig. S8 N_2 adsorption/desorption curves of $FeTiO_3$@C.

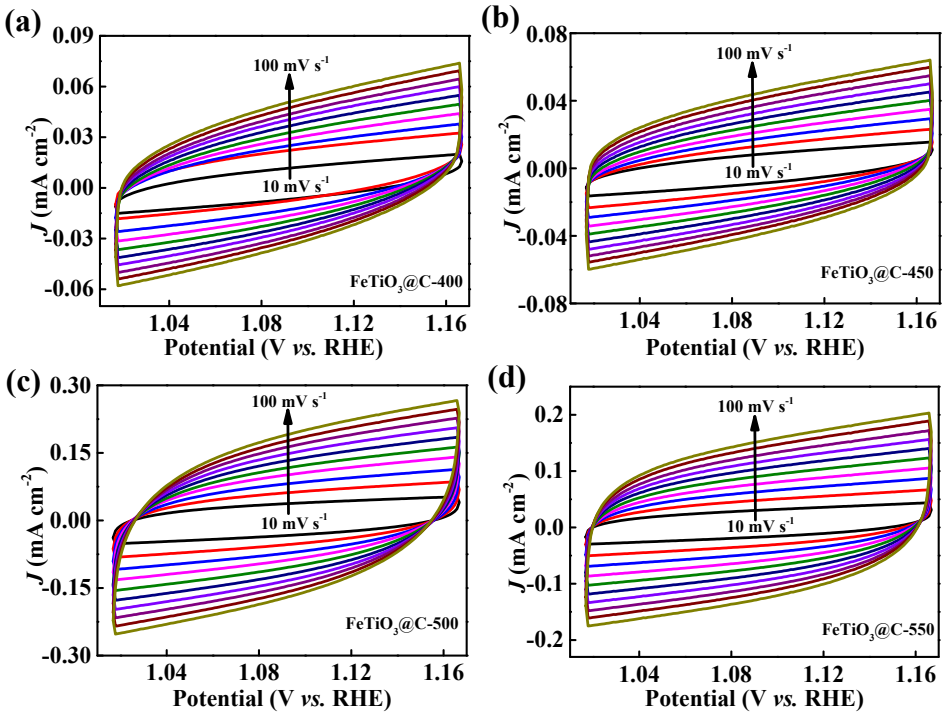

Fig. S9 CV curves of $FeTiO_3$@C-T with the scan rates from 10 to 100 mV/s in the electrochemical double-layer range.

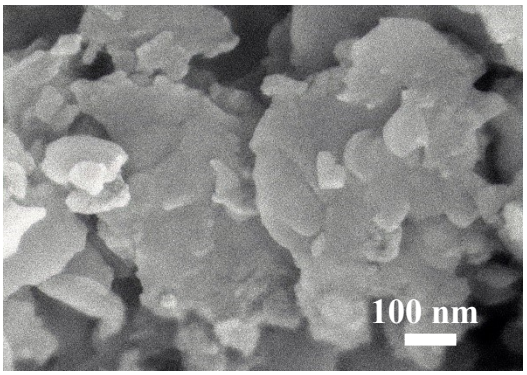

Fig. S10 FE-SEM image for $FeTiO_3$@C after OER stability test.

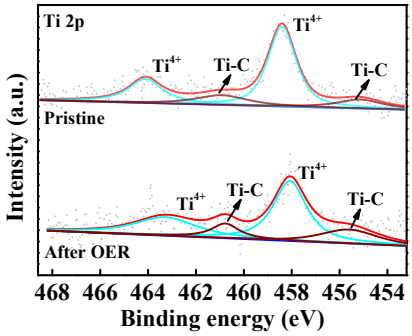

Fig. S11 High-resolution XPS spectra of Ti 2p of $FeTiO_3$@C before and after long-term OER tests.

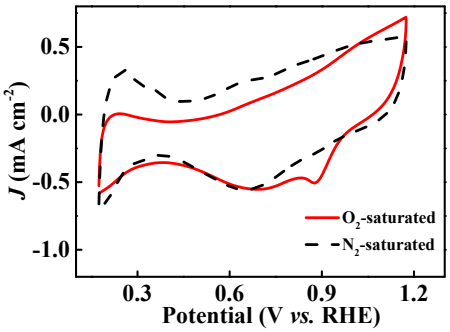

Fig. S12 CV curves of Pt/C in O_2 and N_2-saturated 0.1 M KOH solution.

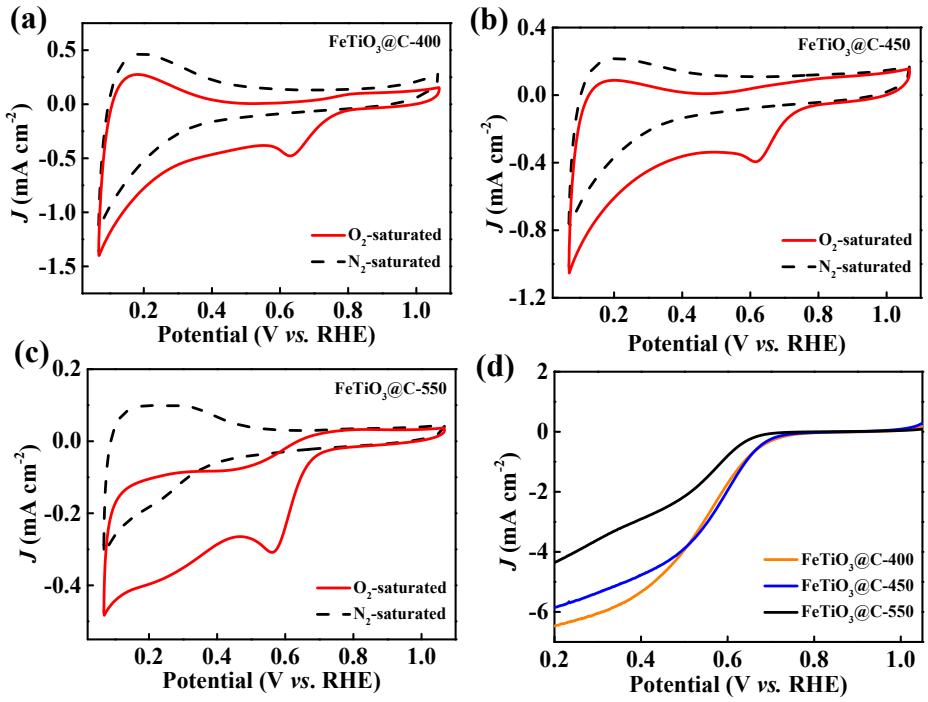

Fig. S13 CV curves of (a) $FeTiO_3$@C-400, (b) $FeTiO_3$@C-450 and (c) $FeTiO_3$@C-550, respectively, in O_2 and N_2-saturated 0.1 M KOH solution. (d) LSVs of $FeTiO_3$@C-T at 1600 rpm.

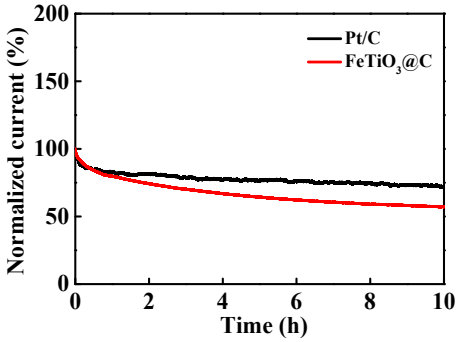

Fig. S14 Chronoamperometric measurements of $FeTiO_3$@C and Pt/C catalysts in O_2-saturated 0.1 M KOH.

Table S1. The ratios of Fe^{3+}/Fe^{2+} of the $FeTiO_3$@C before and after long-term OER tests.

	Area (Fe^{2+})	Area (Fe^{3+})	Ratio (Fe^{3+}/Fe^{2+})
Before long-term OER tests	4255.258	1738.541	0.41
After long-term OER tests	1652.377	2304.026	1.39

Table S2. Comparison of $FeTiO_3$@C with recently reported electrocatalysts for rechargeable Zn-air batteries.

Air catalysts	Power density (mW cm^{-2})	Cycling condition (mA cm^{-2})	Stability	Increased polarization	Date source
$FeTiO_3$@C	**180.5**	**10**	**100h**	**0.15 V**	**This Work**
Fe_3O_4-V_o/N-C	136.8	5	90 h	1.00 V	4
FeP/Fe_2O_3@NPCN	127	5	160h	0.108 V	5
$LaNiO_3$@FeOOH	N.A.	5	900 min	0.09 V	6
$La_{0.7}Ge_{0.3}CoO_3$	160	10	7000 min	0.02 V	7
$LaMnO_3$-CoO	101.48	10	150 cycles	0.26 V	8
$Fe_{0.5}Co_{0.5}O_x$/NrGO	86	10	120 h	0.1 V	9
Co_3O_4@$LaMnO_3$	140	2	185 h	N.A.	10
ZnCo-ZIF@GO	66.6	10	25h	1.05 V	11

Note: N.A. stands for not given.

References

1. X. Wang, J. Wang, J. Qin, X. Xie, R. Yang and M. Cao, *ACS Appl. Mater. Inter.*, 2020, **12**, 39181-39194.
2. Z. Tan, L. Sharma, R. Kakkar, T. Meng, Y. Jiang and M. Cao, *Inorg. Chem.*, 2019, **58**, 7615-7627.
3. S. Liu, Z. Wang, S. Zhou, F. Yu, M. Yu, C. Y. Chiang, W. Zhou, J. Zhao and J. Qiu, *Adv. Mater.*, 2017, **29**, 1700874.

4 Y. Liu, B. Qiao, N. Jia, S. Shi, X. Chen, Z. An and P. Chen, *ChemCatChem*, 2022, **14**, e202101523.

5 K. Wu, L. Zhang, Y. Yuan, L. Zhong, Z. Chen, X. Chi, H. Lu, Z. Chen, R. Zou, T. Li, C. Jiang, Y. Chen, X. Peng and J. Lu, *Adv. Mater.*, 2020, **32**, 2002292.

6 Z. Li, L. Lv, X. Ao, J.-G. Li, H. Sun, P. An, X. Xue, Y. Li, M. Liu, C. Wang and M. Liu, *Appl. Catal. B*, 2020, **262**, 118291.

7 Y. R. Sun, X. Zhang, L. G. Wang, Z. K. Liu, N. Kang, N. Zhou, W. L. You, J. Li and X. F. Yu, *Chem. Eng. J.*, 2021, **421**, 129698.

8 Q. Zheng, Y. Zhang, C. Wang, C. Zhang and Y. Guo, *Energy Fuels*, 2022, **36**, 1091-1099.

9 L. Wei, H. E. Karahan, S. Zhai, H. Liu, X. Chen, Z. Zhou, Y. Lei, Z. Liu and Y. Chen, *Adv. Mater.*, 2017, **29**, 1701410.

10 J. Ran, J. F. Wu, Y. Hu, M. Shakouri, B. Xia and D. Gao, *J. Mater. Chem. A*, 2022, **10**, 1506-1513.

11 Y. Xiao, B. Guo, J. Zhang, C. Hu, R. Ma, D. Wang and J. Wang, *Dalton Trans.*, 2020, **49**, 5730-5735.